JOURNAL OF VIROLOGY, Aug. 2008, p. 7653–7665 Vol. 82, No. 15
0022-538X/08/$08.00+0 doi:10.1128/JVI.00311-08

Varicella-Zoster Virus Open Reading Frame 66 Protein Kinase Is Required for Efficient Viral Growth in Primary Human Corneal Stromal Fibroblast Cells▽

Angela Erazo,[1,2]† Michael B. Yee,[2]† Nikolaus Osterrieder,[4] and Paul R. Kinchington[2,3]*

Graduate Program in Molecular Virology and Microbiology[1] and Departments of Ophthalmology[2] and Molecular Microbiology and Genetics,[3] School of Medicine, University of Pittsburgh, Pittsburgh, Pennsylvania, and Department of Microbiology and Immunology, Cornell University, Ithaca, New York[4]

Received 12 February 2008/Accepted 13 May 2008

Varicella-zoster virus (VZV) open reading frame 66 (ORF66) encodes a serine/threonine protein kinase that is not required for VZV growth in most cell types but is needed for efficient growth in T cells. The ORF66 kinase affects nuclear import and virion packaging of IE62, the major regulatory protein, and is known to regulate apoptosis in T cells. Here, we further examined the importance of ORF66 using VZV recombinants expressing green fluorescent protein (GFP)-tagged functional and kinase-negative ORF66 proteins. VZV virions with truncated or kinase-inactivated ORF66 protein were marginally reduced for growth and progeny yields in MRC-5 fibroblasts but were severely growth and replication impaired in low-passage primary human corneal stromal fibroblasts (PCF). To determine if the growth impairment was due to ORF66 kinase regulation of IE62 nuclear import, recombinant VZVs that expressed IE62 with alanine residues at S686, the suspected target by which ORF66 kinase blocks IE62 nuclear import, were made. IE62 S686A expressed by the VZV recombinant remained nuclear throughout infection and was not packaged into virions. However, the mutant virus still replicated efficiently in PCF cells. We also show that inactivation of the ORF66 kinase resulted in only marginally increased levels of apoptosis in PCF cells, which could not fully account for the cell-specific growth requirement of ORF66 kinase. Thus, the unique short region VZV kinase has important cell-type-specific functions that are separate from those affecting IE62 and apoptosis.

Varicella-zoster virus (VZV) is a highly communicable human alphaherpesvirus that causes chickenpox following a primary infection and herpes zoster (shingles) following reactivation from neuronal latency. Current models (28–30) predict that VZV infects many cell types in the course of primary pathogenesis, including epithelial cells, fibroblasts, keratinocytes, T lymphocytes, dendritic cells, monocytes, and sensory neurons (11, 40). Furthermore, VZV reactivation from latency leads to viral replication in neuronal and nonneuronal cells in the sensory ganglion and in skin tissues at multiple locations belonging to the reactivating dermatome. Reactivation may also lead to VZV replication in ocular tissues. Reactivation involving the ophthalmic division (division V1) of the trigeminal nerve occurs in approximately 10 to 25% of zoster cases, a condition second only in frequency to thoracic zoster (46). It causes herpes zoster ophthalmicus (HZO), a condition that leads to severe ocular diseases in both anterior and posterior compartments, which may ultimately threaten vision (46). Two-thirds of HZO patients report serious ocular complications, most commonly involving the cornea (46). VZV DNA, antigen, and replication have been found in the corneal epithelium at the ocular cell surface, as well as in stromal keratocytes, which sparsely populate the stroma to form an interconnected network in the clear extracellular matrix (42, 65). VZV has also been found in the vitreous fluids and the retinal layers (46, 65). As such, VZV genes affecting viral replication in ocular cell types have important implications for ocular disease.

VZV encodes two serine/threonine (S/T)-specific protein kinases, from open reading frame 66 (ORF66) and ORF47, which have been shown to be dispensable for replication in many cultured cells used for VZV growth (18, 19). Both kinases, however, have important roles that are needed for viral growth in specific cell types (5, 20). Disruption or inactivation of the ORF66 protein kinase leads to minimal impairment of VZV growth in MeWo cells but significant growth defects in T cells, both in culture (60) and in human thymus/liver xenografts in severe combined immunodeficiency (SCID-hu) mice (38, 57, 58). The functional roles directing the growth requirement of ORF66 in T cells are not yet clear. ORF66 affects several host cell processes, including pathways that lead to the downregulation of surface class I major histocompatibility complex-associated antigen presentation (1, 15). In T cells, ORF66 modulates the gamma interferon (IFN-γ)-induced activation of the IFN signaling pathway (58) and inhibits virus-induced apoptosis (57, 58). Apoptosis is also inhibited by ORF66 orthologues (US3 kinases) in several alphaherpesviruses, including herpes simplex virus type 1 (HSV-1), HSV-2, and pseudorabiesvirus (PRV) (3, 4, 12, 43, 45, 49). Loss of ORF66 reduced VZV nucleocapsid production in T cells (58) but did not lead to the accumulation of virions in the nuclear membrane seen in HSV and PRV lacking US3. HSV US3 is thought to be involved in the breakdown of the nuclear lamina to facilitate primary en-

* Corresponding author. Mailing address: Department of Ophthalmology, 1020 EEI building, 203 Lothrop Street, University of Pittsburgh, Pittsburgh, PA 15213. Phone: (412) 647-6319. Fax: (412) 647-5880. E-mail: kinchingtonp@upmc.edu.
† A.E. and M.B.Y. contributed equally to this work.
▽ Published ahead of print on 21 May 2008.

velopment and egress of the nucleocapsid across the nuclear membrane (31, 39, 41). Several additional functions have been attributed to specific US3 kinases, but it is not known if ORF66 shares these functions. These include modulation of the cytoskeletal actin structure (16) and in HSV-1, modification of histone deacetylase function (50).

The only well-characterized target of the ORF66 protein kinase is the IE62 regulatory protein, orthologous to the well-studied HSV ICP4. IE62 is encoded by a diploid gene (ORF62 and ORF71) and is a 1,310-residue phosphoprotein with strong transcriptional transactivator functions. It activates all VZV genes studied to date and can positively or negatively autoregulate its own promoter in transfection assays, depending on the cell type (47, 48). Functions of IE62 are predicted to be similar to HSV-1 ICP4, because IE62 can complement HSV-1 ICP4 deletion mutants and partly replace ICP4 in the context of the HSV-1 genome (13, 17). ICP4 facilitates the recruitment of cellular activating and basal transcriptional factors to viral promoters to enhance RNA polymerase II-mediated transcription (68). In VZV infections, IE62 is at first nuclear but transitions to the cytoplasm as infection progresses and to a predominantly cytoplasmic distribution at late-stage infection. Unlike HSV-1 ICP4, IE62 is an abundant tegument protein incorporated at levels approximately 50% of the major capsid protein (24). Virion packaging requires the ORF66 kinase, as a kinase-negative mutant VZV fails to accumulate IE62 in virions (22, 23). In coexpression studies, ORF66 kinase phosphorylates IE62 directly in vitro at two sites, mapped to serine residues 686 (S686) and S722. IE62 protein containing an S686A mutation does not accumulate in the cytoplasm in the presence of the ORF66 kinase, strongly suggesting that the ORF66 kinase-directed phosphorylation of S686, immediately adjacent to the IE62 nuclear localization signal, drives IE62 exclusion from the nucleus (14, 23, 26). Recent studies have suggested that the ORF66 kinase is not the only means by which IE62 can accumulate in the cytoplasm, since T cells infected with VZV lacking ORF66 kinase still show cytoplasmic forms of IE62 (57). This suggests that a host cell component may be involved in the cytoplasmic accumulation of IE62 in infection.

Recently, we detailed the development of recombinant VZV which express enhanced green fluorescent protein (GFP) tagged to the amino terminus of either functional or truncated ORF66 protein (15). Using these and a VZV expressing a kinase-inactivated ORF66 protein, we show that VZV lacking ORF66 kinase activity fails to grow in primary human corneal stromal fibroblast (PCF) cells. The ORF66 growth requirement is, however, separate from its role in regulating IE62 nuclear import to enable virion packaging. Furthermore, while cells infected with VZV expressing inactivated ORF66 show higher levels of apoptosis in PCF cells, this does not account for the failure of ORF66 kinase-negative VZV to replicate in this cell type. PCF cells represent the first nonlymphocytic cell type in which the kinase has a critical role for VZV replication.

MATERIALS AND METHODS

Cells. MRC-5 cells (human lung fibroblasts; ATCC, Manassas, VA) and MeWo cells (human melanoma cell line; kindly provided by C. Grose, University of Iowa, Iowa City) were maintained and used to grow VZV as described previously (14). PCF cells were derived at the Tissue Culture and Morphology Core Module of the Department of Ophthalmology at the University of Pittsburgh. All primary cells were isolated under protocols approved by the University of Pittsburgh Committee for Oversight on Research Involving the Dead. Briefly, discarded donor rims of human corneas for transplantation were delivered under anonymous conditions. The scleral, endothelial, and epithelial tissues were removed by mechanical debridement using forceps. Washed corneal stroma was cut horizontally to expose internal stromal tissue to medium. Sections were then treated with 1 mg/ml collagenase for 30 s and then washed with 10% fetal bovine serum in Dulbecco's modified Eagle medium before placement into plastic culture dishes overlaid with a glass coverslip. Following incubation at 37°C under medium for 2 to 3 days, cells on the coverslip and plastic support were trypsinized and passaged twice before being mixed with other donor fibroblasts and frozen in aliquots under liquid nitrogen. PCF cells were used in experimental studies within five to nine passages and were maintained in Dulbecco's modified Eagle medium–nutrient mixture F-12 (Ham) (1:1) containing sodium bicarbonate and sodium pyruvate (Invitrogen) supplemented with 10% fetal bovine serum and antibiotic-antimycotic mixture (100 U/ml penicillin G, 100 μg/ml streptomycin, and 0.25 μg/ml amphotericin B [Fungizone]; Gemini Bio-Products).

VZV and derivation of rVZV. The VZV used here is based on the parent of the Oka vaccine strain (pOka). The construction and derivation of VZV.GFP-66 and VZV.GFP-66s from pOka-based cosmids have been detailed previously (15). These express amino-terminal GFP-tagged functional ORF66 protein or one that has been disrupted by insertion of stop codons at residue 84, respectively. The same cloning procedure detailed in that study was used to derive VZV.GFP-66kd, which contains GFP-tagged ORF66 protein with two highly conservative changes in the catalytic loop domain of the kinase (D206E, K208R) (23). The derivation of a rescuant VZV was carried out by subcloning a unique SgrAI-AvrII fragment from the pSpe23 cosmid that was used to derive VZV.GFP-66kd into a modified pUC19 derivative containing sites for SgrAI and AvrII (15). The AvrII-BamHI fragment within this construct that contains the ORF66 promoter and amino-terminal portion of ORF66 with the inactivating mutations was replaced with the same corresponding DNA fragment containing functional GFP-tagged ORF66 (15). The SgrAI-AvrII fragment was then reengineered back into the pSpe23 cosmid to generate pSpe23GFP66rsc, which was then used in conjunction with pFsp73, pSpe14, and pPme2 to derive a recombinant VZV (rVZV) designated VZV.GFP-66Rsc.

Additional rVZV constructs were derived from viral DNA cloned as a bacterial artificial chromosome (BAC) containing the entire pOka genome (62). To generate S686A changes in ORF62 and ORF71, we conducted mutagenesis using the markerless two-step recombination system, detailed previously (63). All oligonucleotides were obtained from IDT, Inc. (Coralville, IA) and were purified by sodium dodecyl sulfate-polyacrylamide gel electrophoresis (SDS-PAGE) by IDT. PCR was performed with Expand proofreading polymerase (Roche Diagnostics, Indianapolis, IN). The two oligonucleotides used for mutagenesis were S686AF (5′-GTGTGTCCACCGGATGATCGTTTACGAACTCCGCGCAAG CGCAAGGCTCAACCGGTCGAGAGCAGAAGCCTCCTCGACAAAGGA TGACGACGATAAGTAGGG-3′) and S686AR (5′-CGACGGGTGTCTCCC TAATCTTGTCGAGGAGGCTTCTGCTCTCGACCGGTTGAGCCTTGCG CTTGCGCGGAGTTCGTAAACAACCAATTAACCAATTCTGATTAG-3′) (underlined residues mark the altered sequence discussed in the text). The two oligonucleotides were used to PCR amplify the kanamycin resistance cassette (Kan^r) from the plasmid pEP-kanS2 (63) to add the IE62 flanking sequences required for homologous recombination and mutagenesis. The gel-purified PCR product was then electroporated into *Escherichia coli* SW105 (a kind gift of N. Copeland, NCI, Frederick, MD) containing the pOka VZV BAC. Recombination was induced by heating to 42°C for 15 min, and growth and selection of recombinants were done by plating at 32°C on LB agar plates containing 15 μg/ml kanamycin and 25 μg/ml chloramphenicol (Chm). DNA of individual colonies was mapped for the correct insertion of the cassette (the first recombination occurred in ORF71) by restriction analysis using HindIII digestion. Resolution of the construct to remove the Kan^r cassette was achieved by transformation of the plasmid pBAD-I-SceI into SW105 cells containing the modified VZV BAC, which was then growth selected on LB agar plates additionally containing 50 μg/ml ampicillin. I-SceI expression was induced by growth in liquid culture containing 1% arabinose, and a second round of recombination was induced by heating cultures to 42°C for 15 min. Colonies growing at 32°C on LB agar containing Chm, Amp, and arabinose were checked for loss of the Kan^r cassette by replica plating individual colonies onto plates containing kanamycin. *Escherichia coli* cells containing the altered BAC were then subjected to a second round of mutagenesis with the same PCR fragment, selecting for homologous recombination into ORF62. The BAC DNAs were transfected into MeWo cells using Lipofectamine 2000 (Invitrogen, Carlsbad, CA), and derived VZV plaques were visible after 3 to 5 days of incubation at 35°C. VZV containing a single

change in ORF71 was termed VZV.71.S686A, whereas rVZV with mutations in both IE62 genes was termed VZV.IE62(S686A)[2]. The insertion of AgeI sites into both genes was confirmed by restriction analyses. The verification of the presence of the changes in VZV was carried out through Southern blotting of AgeI-digested infected cell genomic DNA, purified from VZV-infected MeWo cells using Qiagen's blood and cell culture DNA midi kit (Valencia, CA), onto a positively charged nylon membrane (Nytran SuPerCharge; Schleicher & Schuell, Keene, NH). The 1,018-bp fragment isolated from an AgeI digest of pKCMV62 DNA was used as a probe following radiolabeling with [α-^{32}P]dCTP (Perkin-Elmer, Waltham, MA) and the random prime labeling kit (Roche Diagnostics Corp., Indianapolis, IN).

Antibodies and immunological procedures. Rabbit polyclonal antibodies to IE62 (14, 15, 23) and to VZV proteins from ORFs 4, 61, and 63 were detailed previously (21). Previously detailed anti-peptide antibodies to ORFs 10 (21) and 29 (25) were also used in this work. Antibodies to ORF9 (8) were a kind gift of W.T. Ruyechan, SUNY at Buffalo, NY, and antibodies to ORF47 (44) were a kind gift of C. Grose (University of Iowa, Iowa City). Mouse antibodies to β-actin (Sigma, St. Louis, MO) and to ORF40 major capsid protein (MCP; Virusys Corp., Sykesville, MD) were purchased commercially. All immunofluorescent staining procedures were carried out as described previously (15), and antibodies were detected using goat anti-rabbit immunoglobulin G antibody conjugated to Alexa Fluor 546 or goat anti-mouse immunoglobulin G antibody conjugated to Alexa Fluor 488 (15). Immunofluorescence was visualized using a Nikon Eclipse TE2000-E epifluorescence microscope equipped with a xenon lamp.

Analysis of viral growth. VZV for growth rate studies was prepared from aliquoted and titrated stocks of virus in MeWo cells stored in liquid nitrogen. Stocks were 80 to 95% infected at the time of preparation, to minimize addition of uninfected cells. Viral growth rates were determined using similar procedures detailed elsewhere (15). Briefly, confluent monolayers of cells were established and infected with cell-associated VZV at an estimated 300 infectious centers (IC) per well. Serial dilutions of the infecting virus were immediately titrated on MeWo cell monolayers to determine the exact titer of the inoculum. At specific times, cells were trypsinized, diluted in fresh medium, and added to fresh MeWo monolayers. At 4 to 5 days postinfection (p.i.), plaques were quantified either by using autofluorescence of GFP or by immunofluorescent staining for IE62. Statistical analysis to compare overall growth curves was done using Dunnett's multiple comparison test using GraphPad Prism software v. 4.0. For growth curve enumeration by flow cytometry, a similar setup was established, except that trypsinized cells were immediately fixed in 1% paraformaldehyde, washed in 1× phosphate-buffered saline (PBS), and counted using a FACSaria cytometer cell sorter (Becton-Dickinson). GFP gates were set using mock-infected cell controls.

Virion purification and characterization. Virion purification was performed as described previously (21). Briefly, monolayers of MeWo cells infected with VZV were grown at 35°C until showing ~80% cytopathic effect. Harvested cells were washed with ice-cold PBS containing a protease inhibitor cocktail (Complete EDTA-free; Roche Diagnostics, Indianapolis, IN) and subjected to Dounce homogenization to obtain cytoplasmic extract. Virion particles were also collected from the cell-free medium by high-speed centrifugation and combined with cytoplasmic fractions. Virions were purified by velocity gradient ultracentrifugation for 2 h at 17,000 × *g* on 5 to 15% Ficoll gradients made in PBS. The diffuse virion band migrating approximately two-thirds down the tube was harvested, concentrated by centrifugation, and resuspended overnight at 4°C in PBS containing protease inhibitors. Virions were then subjected to 10 to 50% sucrose gradients made in PBS, which were then fractionated using a piston gradient fractionator. For protein analyses, proteins were precipitated from the fractions with 10% trichloroacetic acid, washed with ice-cold acetone, and resuspended in 100 μl protein gel loading buffer for SDS-PAGE. For immunoblotting, proteins were separated by SDS-PAGE, transferred to Immobilon-P membrane (Millipore, Billerica, MA), and probed with rabbit polyclonal antibodies to ORF10 to identify the peak virus fractions. These were pooled for further studies for VZV proteins. Virion samples for protein staining were run on 4 to 15% Tris-HCl linear gradient polyacrylamide-SDS gels (Bio-Rad Laboratories, Hercules, CA) and stained with Sypro ruby protein gel stain (Invitrogen, Carlsbad, CA). Proteins were visualized using a Bio-Rad Fluor-S MultiImager.

Apoptosis assay. Confluent cells were seeded onto six-well plates and infected with VZV at a multiplicity of infection (MOI) of approximately 0.02 or mock infected. At the times indicated, cells were harvested and stained according to the manufacturers' instructions for allophycocyanin (APC)-Annexin V (BD Pharmingen). Briefly, cells were washed twice in cold PBS, resuspended in the supplied binding buffer, and counted. Approximately 1×10^5 cells were then stained with APC-Annexin V and 7-amino-actinomycin D (7-AAD). Stained cells were analyzed by flow cytometry, and GFP gates were set using mock-infected cell controls. Cells were characterized and analyzed using BD FACS-Diva v4.1 software. Experimental values are the fraction of GFP-positive cells showing APC-Annexin V-positive staining as a percentage of the total GFP-positive cells. Values represent the means of three identical experiments. Statistical analysis was done with Student's *t* test using GraphPad Prism software v4.0.

RESULTS

ORF66 is required for efficient growth of VZV in PCF cells. The VZV ORF66 protein kinase is categorized as a nonessential gene in culture, yet recent studies indicate it is needed for VZV growth in T cells (28, 57, 58). To explore the growth properties of VZV with or without ORF66 kinase in other cell types, we employed two fluorescent VZV recombinants, detailed previously (15), which express a GFP-tagged and functional ORF66 protein or one that is disrupted at residue 84. GFP has no apparent effect on VZV growth when compared to parent pOka virus (15). We also generated VZV which expressed the full-length ORF66 protein but in which the kinase was inactivated by two point mutations in the catalytic loop (VZV.GFP-66kd), as well as a rescuant of this change (VZV.GFP-66Rsc) in which the two point mutations were reversed. These mutations abrogated the ability of ORF66 to induce accumulation of cytoplasmic IE62 or phosphorylate IE62 peptides in coexpression assays (23). The rescuant was phenotypically indistinguishable from VZV.GFP-66 and parental Oka in all assays in which it was examined.

IE62 produced by viruses expressing functional ORF66 protein in both MRC-5 cells (Fig. 1A) and PCF cells (Fig. 1B) showed predominantly cytoplasmic forms in most GFP-positive cells (Fig. 1A and B, panels a, c, j, and l). In contrast, IE62 expressed by VZV.GFP-66kd and VZV.GFP-66s displayed a predominantly nuclear localization in both cell lines in GFP-positive cells (Fig. 1A and B, panels d, f, g, and i). GFP-66s showed a diffuse cellular localization (Fig. 1A and B, panels h and i), but GFP-66kd protein exhibited a distinct predominantly nuclear localization in both cell lines (Fig. 1A and B, panels e and f) that was clearly different from functional kinase produced by VZV.GFP-66, suggesting that the kinase activity of ORF66 affected its cellular localization. Some cells displayed marked nuclear rim accumulation of GFP-66kd.

In addition to differences in cellular distribution patterns, it was obvious that ORF66-negative VZV formed tiny plaques on PCF cells that involved far fewer cells. In MRC-5 cells, plaque size of all four viruses increased in size during the duration of the study (up to 7 days postinfection), although plaques of VZV not expressing kinase were slightly smaller (data not shown). In PCF cells, plaques of the VZV lacking the kinase formed very small centers of infection at day 1 to 2 that involved 10 to 20 cells, but these failed to increase further in size, suggesting that infections were initially established but failed to progress. We also found severe growth impairment of a previously described ORF66 kinase-deficient VZV made in the vaccine Oka background (19). To quantify this more accurately, we determined yields of progeny virus on both cell types for all four viruses. In MRC-5 cells, VZV virions without the kinase were marginally impaired for virus growth compared to VZV.GFP-66, yielding a 0.4- to 0.7-log reduction at 96 h p.i. (Fig. 2A). Maximal titers of VZV.GFP-66s and VZV.GFP-66kd were lower (7.5×10^3 and 4.8×10^3 IC, respectively) than those of VZV.GFP-66 (2.0×10^4 IC) and VZV.GFP-66Rsc

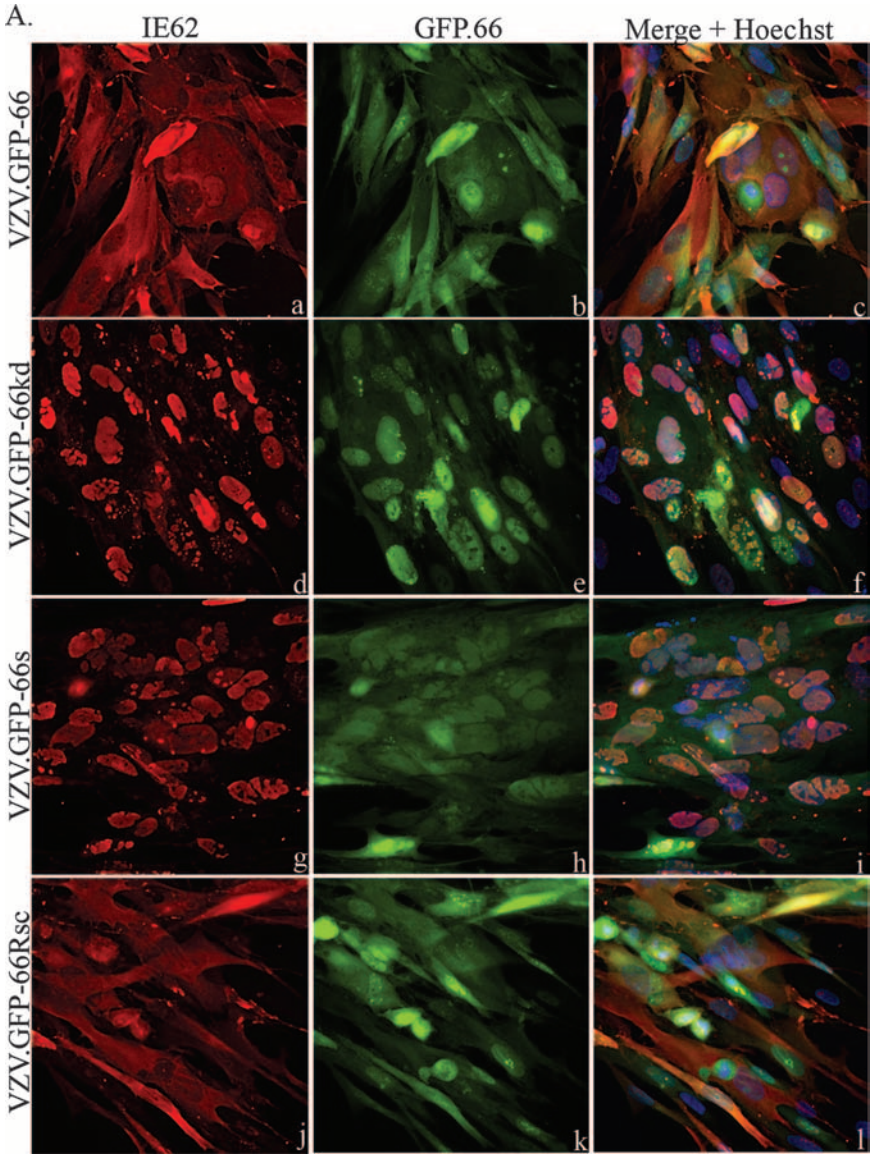

FIG. 1. IE62 cellular distribution and GFP expression in VZV-infected cells. MRC-5 cells (A) or PCF cells (B) were infected at an MOI of 0.0005 with MeWo cell-grown VZV.GFP-66 (a to c), VZV.GFP-66kd expressing complete GFP-tagged kinase-inactivated ORF66 protein (d to f), VZV.GFP-66s expressing GFP tagged to residues 1 to 84 of ORF66 (g to i), or VZV.GFP-66Rsc (j to l). Cells were fixed with 4% paraformaldehyde at 3 days p.i. and immunostained with rabbit anti-IE62, which was then detected with anti-rabbit Alexa Fluor 546 (a, d, g, and j). ORF66 expression was determined using GFP autofluorescence (b, e, h, and k). The merge panels (c, f, i, and l) are overlays of GFP (green), IE62 (red), and nuclei stained with Hoechst dye (blue). Fluorescence images were taken using a 40× objective.

(2.2×10^4 IC) at 96 h p.i. However, the overall growth curve differences compared to VZV.GFP-66 were not statistically significant ($P > 0.05$). In contrast, a much greater impairment for growth of ORF66-negative viruses was observed in PCF cells. While VZV.GFP-66 and VZV.GFP-66Rsc reached maximum titers of 3.2×10^4 and 4.0×10^4 IC, respectively, at 96 h p.i., VZV.GFP-66s and VZV.GFP-66kd maximal titers peaked at 48 h (1.1×10^3 and 4.3×10^2 IC, respectively) and declined thereafter (Fig. 2A). Extension of the growth curves to 7 days did not lead to any increases in viral titer (data not shown). These results indicate that PCF cells do not permit efficient growth of VZV if the ORF66 kinase is not functional.

The growth impairment in PCF cells was also detected when flow cytometry was used to quantify GFP-positive cells as an indicator of infection. In MRC-5 cells infected with VZV.GFP-66, greater than 40% of cells showed GFP-positive signals by day 9 p.i. (Fig. 2B). ORF66 kinase-negative viruses showed a reduced rate of increase in the number of GFP-positive cells, with VZV.GFP-66kd showing marginally greater impairment. However, in PCF cells, VZV with nonfunctional kinase showed only a very small increase in the number of GFP-positive cells at day 1, which then subsequently diminished. VZV.GFP-66 infection resulted in a reduced rate of increase of GFP-positive cells compared to that seen in MRC-5 cells, but this reflects a slightly reduced growth rate in PCF cells (compare with Fig. 2A) rather than a loss of GFP-positive cells in flow cytometry.

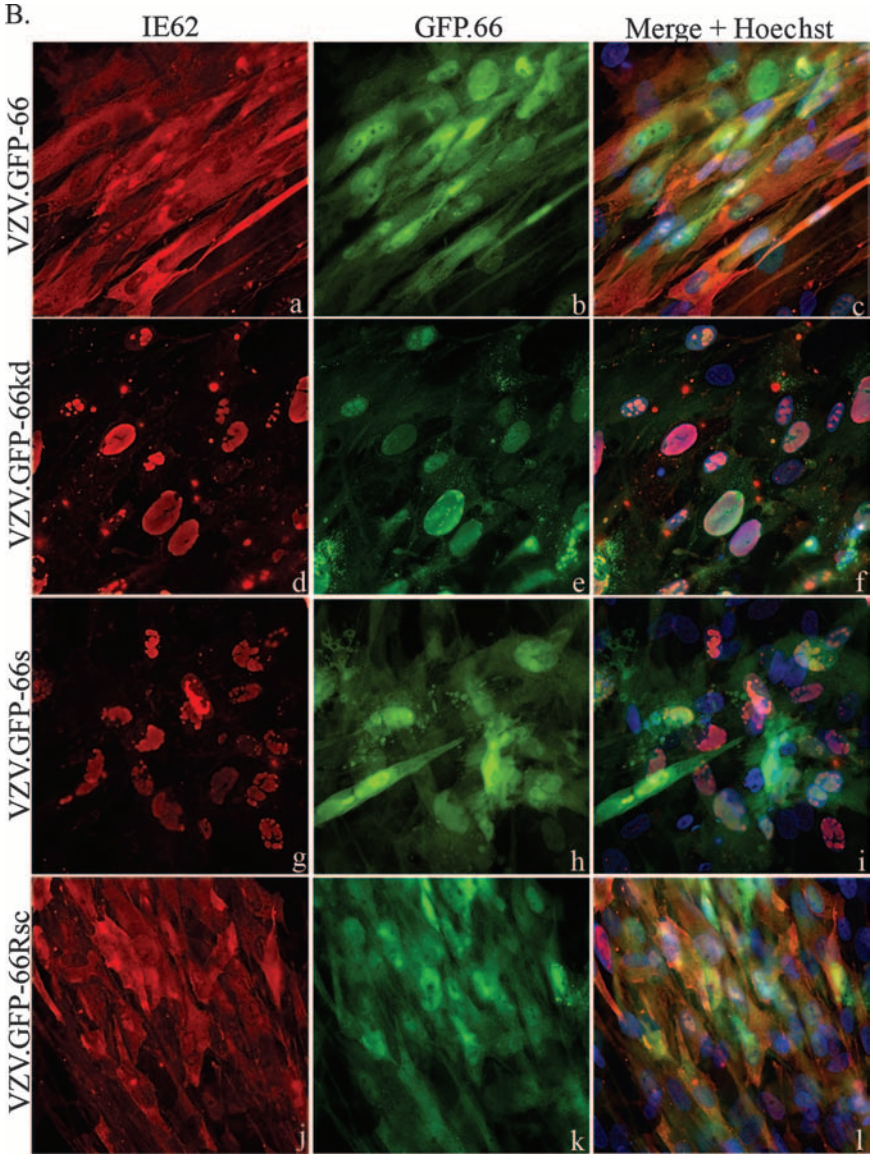

FIG. 1—*Continued.*

We did not find there was significant loss of cell structure due to mechanical damage in these studies. Thus, these results reflect growth curve studies and further establish that PCF cells are unable to support VZV replication in the absence of functional ORF66 protein kinase.

Derivation of VZV expressing IE62 protein mutated at the critical ORF66 phosphorylation site. The most well-characterized target of the ORF66 kinase is IE62, the VZV major regulatory protein. In transfection studies, IE62 expressed alone is largely nuclear, but when it is coexpressed with the ORF66 kinase, IE62 accumulates predominantly in the cytoplasm. We have previously shown that the accumulation of cytoplasmic IE62 requires the ORF66 kinase activity and that the kinase phosphorylates IE62 both in vivo and in vitro at two residues, S686 and S722. However, IE62 containing S686A changes (but not IE62 containing the S722A mutation) was resistant to ORF66-induced cytoplasmic accumulation and remained predominantly nuclear in cells expressing the ORF66 protein kinase (14). While it was concluded that ORF66 kinase phosphorylated IE62 at residue S686 to induce its cytoplasmic accumulation, the interaction has not been addressed in the context of VZV infection. It is clear that VZV-infected cells not expressing the ORF66 kinase show only nuclear IE62 (Fig. 1A and B) and loss of the kinase abrogates virion packaging of the IE62 protein (14, 22, 24). Thus, it was possible that the requirement of the kinase in PCF cells reflected a loss of the cytoplasmic accumulation and virion packaging of IE62.

To test this possibility, we developed recombinant VZV in which the IE62 residue targeted by the kinase, S686, was altered to alanine [VZV.IE62(S686A)^2]. Our previous studies (14) predicted that IE62 with this change would not be regulated by the ORF66 kinase during VZV infection. The mutations were generated in a VZV pOka BAC (62) and were designed to simultaneously introduce a marker AgeI site with

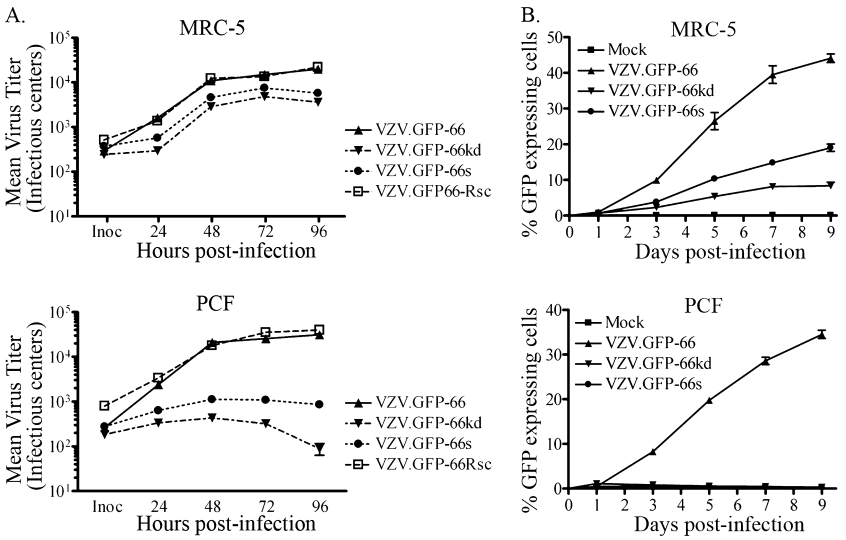

FIG. 2. Progeny virus growth curves reveal a requirement for ORF66 for VZV growth in PCF cells. (A) Growth curves were performed as detailed in Materials and Methods, and the titers of the progeny VZV in MRC-5 cells (top) and PCF cells (bottom) are shown. Confluent monolayers were infected at an MOI of 0.001 with VZV.GFP-66, VZV.GFP-66kd, VZV.GFP-66s, or VZV.GFP-66Rsc. The inoculum (Inoc) of each virus was immediately determined upon the setup of the studies at time 0 h. At 24, 48, 72, and 96 h postinfection, infected cells were trypsinized and titrated onto subconfluent monolayers of MeWo cells. Plaque formation and enumeration were assessed by fluorescence microscopy at 4 to 5 days postinfection. The *x*-axis values represent hours postinfection when cells were harvested, and *y*-axis values represent average total numbers of infectious centers at each time point. Each data point was determined in quadruplicate, and results represent the means ± standard errors of these values. (B) GFP-positive infected cell numbers fail to increase in PCF cells if the ORF66 protein is disrupted. MRC-5 cells (top) or PCF cells (bottom) in confluent monolayers in 35-mm dishes were infected with VZV.GFP-66, VZV.GFP-66kd, or VZV.GFP-66s at an MOI of 0.001 or mock infected. On the indicated day after infection indicated (*x* axis), cells were harvested and counted by flow cytometry, gating for GFP-positive cells. The ratio of GFP-positive cells to the total number of cells in the harvested monolayers is expressed as a percentage (*y* axis). Values represent the means ± standard errors of three parallel but independent values.

the S686A mutation (Fig. 3A). In the parental BAC, AgeI digestion produced a 2 M 1,018-bp fragment, representing an internal fragment of ORF62 and ORF71 (Fig. 3B). DNA of BACs engineered to contain the S686A mutation in only the ORF71 gene showed a loss of one copy of the 1,018-bp fragment, while DNA from BACs containing S686A mutations in both the ORF62 and ORF71 genes showed loss of both 1,018-bp fragments (Fig. 3B). The introduction of the mutation resulted in the generation of two smaller AgeI DNA fragments of 605 and 413 bp. While these could not be easily identified in ethidium bromide-stained gels (Fig. 3B) due to their small size and comigration with other DNA fragments, we confirmed their presence by Southern blot analyses. Viruses derived from each BAC were used to generate infected cell DNA, and AgeI digests were examined by Southern blotting and probing with a radiolabeled 1,018-bp AgeI DNA fragment (Fig. 3C). As expected, a prominent 1,018-bp fragment was detected in pOka, one copy was reduced to 605 and 413 bp fragments in VZV with the ORF71 mutation, and both copies were converted to the smaller fragments in DNA of VZV.IE62(S686A)^2. VZV with single and double copies of the S686A mutations grew and formed plaques that were similar in size and appearance to that formed by BAC-derived pOka VZV in MeWo cells. We then confirmed the presence of the S686A mutations by DNA sequencing.

VZV.IE62(S686A)^2 IE62 remains nuclear in the presence of functional ORF66. The prediction was that IE62 expressed from VZV.IE62(S686A)^2 would remain nuclear throughout viral infection, because IE62 could not be phosphorylated by the ORF66 protein kinase at the site affecting its cellular distribution (14). While VZV.GFP-66 formed abundant cytoplasmic forms of IE62 in MeWo cells, VZV.IE62(S686A)^2 expressed IE62 that remained exclusively nuclear at all stages of infection, even in cells expressing the late ORF40 major capsid protein (Fig. 4A). VZV.71.S686A produced IE62 that showed an intermediate phenotype (data not shown). Extension of these studies to MRC-5 and PCF cells revealed that IE62 remained exclusively nuclear in both cell types, fully overlapping the Hoechst nuclear stain (Fig. 4B). Thus, it is clear that residue S686 of IE62 is critical for ORF66 to regulate IE62 nuclear import in the context of viral infection of several cell types.

The predominantly nuclear localization of IE62 in VZV. IE62(S686A)^2-infected cells is similar to that seen for ORF66 kinase-negative VZV. To confirm the integrity of the ORF66 protein kinase, we sequenced the ORF and its promoter and also evaluated the ORF66 gene in VZV.IE62(S686A)^2 by PCR amplifying it, placing it into an expression vector, and then examining it for the ability to induce cytoplasmic forms of IE62 in coexpression studies. As the kinase retained the ability to regulate the cellular localization of IE62 (data not shown), we conclude that the exclusively nuclear phenotype of IE62 was due to a loss of the IE62 S686 site rather than a spurious kinase-inactivating mutation in the ORF66 protein.

Tegument proteins of VZV.IE62(S686A)^2. Previous studies demonstrated that genetic disruption of the ORF66 kinase in VZV resulted in the IE62 protein remaining completely nuclear throughout infection and simultaneously abrogated the

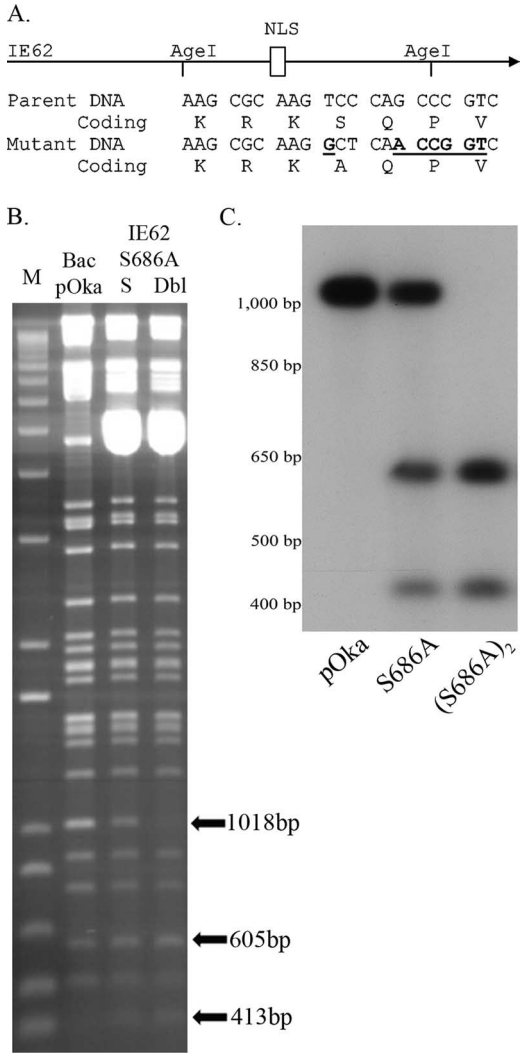

FIG. 3. DNA characterization of BAC DNA and of VZV-infected cell DNA of the recombinants VZV.71.S686A and VZV.IE62(S686A)^2. (A) Schematic representation of the mutagenesis of IE62 residue S686. The top portion represents IE62 and its nuclear localization signal (NLS), with the presence of the existing AgeI sites shown. Part of the DNA sequence and encoded amino acids of the target region in the parental DNA and in mutant DNA are shown underneath. The DNA sequence of the alterations induced by mutagenesis that introduce the novel AgeI site is underlined. (B) A 1.2% agarose gel showing DNA fragments generated by AgeI digestion of the VZV BAC DNAs derived from pOka and BACs containing the mutation in ORF71(S) or in both ORF62 and ORF71 (Dbl). M is the DNA size marker (1Kb plus; Invitrogen). The abundant 5-kbp DNA seen in the mutant BACs represents the pBAD-*I-SceI* plasmid used to select for loss of the Kan^r cassette. The positions of the 1,018-bp fragment in the pOka BAC and the resultant smaller digestion fragments in the mutants are shown by arrows. (C) Southern blot of rVZV-infected MeWo cell genomic DNA, digested with AgeI and probed with a [α-^{32}P]dCTP-labeled 1,018-bp fragment obtained from an AgeI digest of pKCMV62. The autoradiograph shows DNA of VZV pOka, VZV.71.S686A, and VZV.IE62(S686A)^2. The approximate sizes of DNA markers are indicated to the left.

packaging of IE62 into virions, leading us to conclude that the cytoplasmic distribution of IE62 during infection was required for its virion packaging (22). The predominantly nuclear IE62 seen in VZV.IE62(S686A)^2-infected cells would also be predicted to abrogate IE62 packaging into VZV.IE62(S686A)^2 virions. To examine this possibility, we infected MeWo cells with VZV.IE62(S686A)^2 or VZV.GFP-66 and used methods established previously to obtain purified virions from the cytoplasmic extracts (22). We consistently obtained lower levels (approximately one-third to one-fifth) of VZV.IE62(S686A)^2 virions compared to virions obtained from VZV.GFP-66 infected cells, based on total protein content of the Ficoll gradient-purified virion fraction, although virion bands migrated to the same relative position in the gradients. Comparison of Ficoll gradient-purified virions to cell extracts of VZV.GFP-66 (Fig. 5A) showed that virions contained a prominent polypeptide of 155 kDa, the major capsid protein, and had a virion protein profile that was similar to that previously reported (22). We noted that two polypeptides of 175 kDa and 180 kDa seen only in infected cell extracts (Fig. 5A) were the same size as the predominant forms of IE62 seen in infected cells (22). Comparison of 15% of the total Ficoll gradient virion preparations from VZV.GFP-66 with 30% of the total virion preparation from VZV.IE62(S686A)^2-infected cells revealed that both virions had similar protein profiles, with the exception that the 175-kDa polypeptide was not seen in VZV.IE62(S686A)^2 virions. This is the size of virion-packaged IE62 reported previously (22).

To further assess virion protein content, virions were then purified on sucrose gradients, which were subsequently fractionated. Fractions containing virions (identified by probing SDS-PAGE-separated proteins in each fraction for ORF10 protein) were restricted to three fractions from the central region of each gradient. The total protein stain for VZV.GFP-66 virions was highly similar to that seen from the Ficoll gradient, although the low levels of virions obtained for VZV.IE62(S686A)^2 did not permit a total protein comparison. It is possible that virions produced by VZV.IE62(S686A)^2 may have reduced stability, although this has not been investigated further. Based on the levels of the ORF10 major tegument protein, proteins of the sucrose gradient-purified virions were normalized and probed for additional VZV proteins. The absence of nonstructural proteins encoded by ORF29 (the homologue of HSV ICP8, which is also nonstructural) and ORF61 established that the preparations were not contaminated with infected cell material (Fig. 5B). Virions of VZV.IE62(S686A)^2 showed no reactivity to IE62-specific antibodies, although IE62 was present in VZV.GFP-66-infected whole-cell extracts and virions. This supports the conclusions that the major immediate early regulatory protein is not packaged into VZV.IE62(S686A)^2 virions and that virion packaging of IE62 requires IE62 localization to the cytoplasm.

The VZV tegument contains additional VZV regulatory proteins encoded by ORFs 4, 10, 47, and 63 (21, 24, 61). The ORF9 protein, which has recently been shown to interact with IE62, is also a suspected structural protein, based on its orthologue, the major tegument protein VP22 in HSV-1 (8). We conjectured that the abrogation of cytoplasmic IE62 accumulation may also impair the tegument incorporation of some of these proteins, particularly the proteins encoded by ORFs 4, 9, 47 and 63, which are known to physically interact with IE62. Probing of blots of ORF10-normalized virion proteins of VZV.GFP-66 and VZV.IE62(S686A)^2 revealed that ORF4 and ORF47 proteins were present at similar levels for each virus (Fig. 5B). The ORF9 protein was incorporated into virions as predicted, and multiple forms of the protein were seen in both

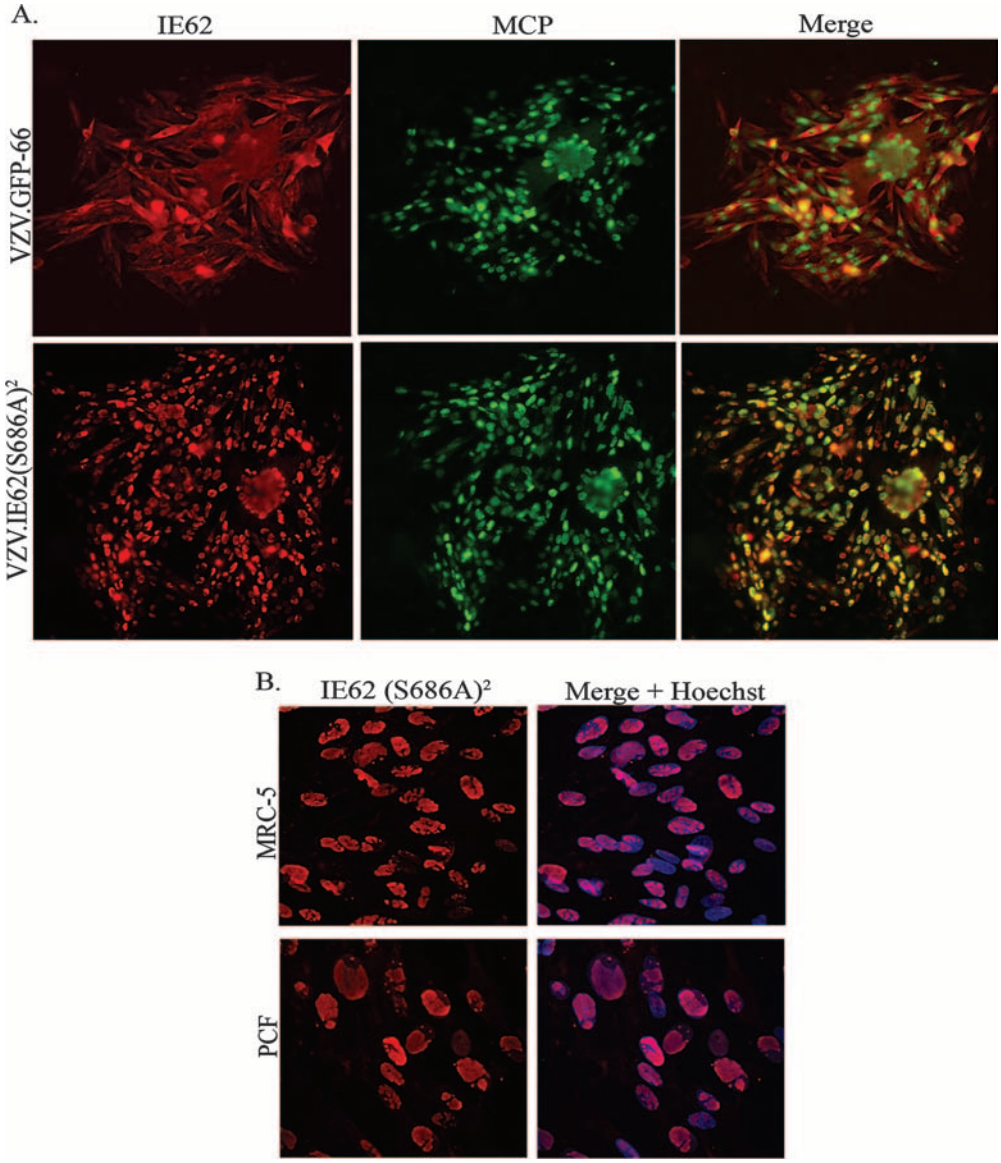

FIG. 4. IE62 localizes to the nucleus in VZV.IE62(S686A)^2-infected cells. (A) Scanned images of VZV.GFP-66 and VZV.IE62(S686A)^2-infected MeWo cell plaques, immunostained with rabbit anti-IE62 and mouse anti-MCP antibody, which were then detected with anti-rabbit Alexa Fluor 546 or anti-mouse Alexa Fluor 488, respectively. The merge panels are overlays of IE62 (red) and MCP (green). (B) Immunofluorescence images of VZV.IE62(S686A)^2-infected MRC-5 (top row) or PCF cells (bottom row) immunostained for IE62 (red). Nuclei detected using Hoechst stain (blue) are displayed in the merged images. All cells were fixed at 3 days p.i. with 4% paraformaldehyde, and images were taken using a 40× objective.

infected cell extracts and in virions. Interestingly, we consistently observed from two studies that VZV.IE62(S686A)^2 virions exhibited increased levels of ORF9 and ORF63 proteins. Interestingly, we did not detect actin as a component of VZV virions from either virus. From this work, we conclude that the mutation of S686A in both copies of IE62 abrogated the incorporation of IE62 into virions. While virion packaging of other tegument-associated regulatory proteins did not require virion IE62, some appeared to compensate for the absence of tegument IE62.

Growth comparisons of VZV.IE62(S686A)^2 and rVZV lacking functional ORF66 in PCF cells. The previous data established that VZV.IE62(S686A)^2 showed a similar phenotype to VZV deficient in functional ORF66. However, comparative reassessment of growth curves of VZV.IE62(S686A)^2 revealed differences to VZV.GFP-66kd and VZV.GFP-66s in PCF cells (Fig. 6). Specifically, by 96 h p.i., VZV.IE62(S686A)^2 grew to titers in PCF cells (2.2×10^3 IC) that were only marginally lower than those of VZV.GFP-66 (5.2×10^3 IC). In contrast, VZV.GFP-66s and VZV.GFP-66kd showed little increase in progeny virus titers subsequent to 24 h p.i., and at 96 h p.i, titers were 3.4×10^1 and 7.3×10^1 IC, respectively. The difference between titers of ORF66-negative viruses and VZV.GFP-66 was statistically significant ($P < 0.01$), mirroring the results shown in Fig. 2A. As VZV.IE62(S686A)^2 clearly replicated in PCF cells, we conclude that the critical

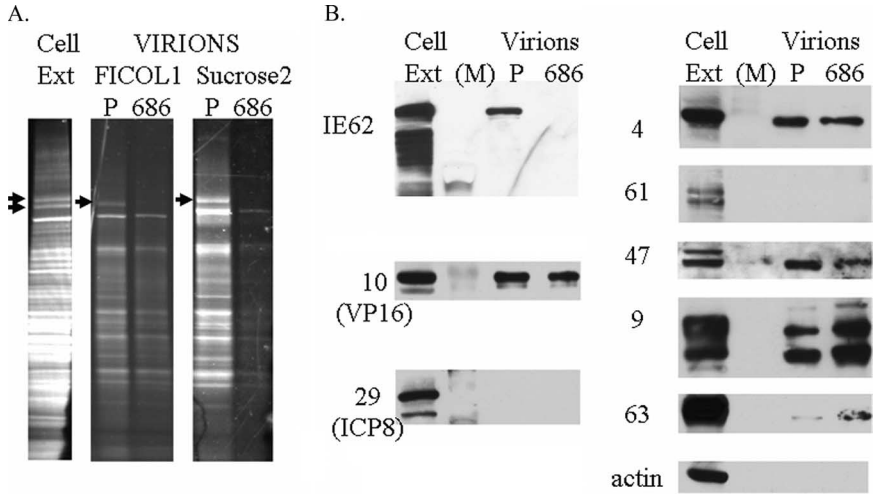

FIG. 5. VZV.IE62(S686A)^2 does not incorporate IE62 into the virion tegument. (A) Sypro ruby staining of purified VZV virion particles harvested from infected MeWo cells following separation on a 4 to 15% Tris-HCl linear gradient SDS gel. A MeWo-infected cell extract is also shown (cell ext), with arrows indicating two suspected forms of IE62. Virion particles were obtained from cells infected with VZV.GFP-66 (P) or VZV.IE62(S686A)^2 (686). Virions are shown following purification after the 5 to 15% Ficol gradient step (Ficol 1) and after the second fractionation on 10 to 50% sucrose gradients (Sucrose2). Arrows depict the 175-kDa protein in the VZV.GFP-66 virion fractions. (B) Immunoblot analysis of cell extracts and sucrose gradient-purified virions that were equalized based on the abundance of ORF10 protein and then probed with rabbit antibodies to VZV proteins derived from ORFs 4, 9, 10, 29, 47, 61, 62, and 63 and β-actin. The HSV homologues of some VZV proteins are indicated in brackets. M indicates the marker lane.

ORF66 function required for productive VZV growth in PCF cells is independent of its functions in regulating IE62 nuclear import through phosphorylation of the IE62 S686 site. We presume that virions produced in PCF cells by VZV.IE62(S686A)^2 and by ORF66 kinase-negative VZV do not incorporate IE62 in VZV virions, as IE62 would not localize to the site of tegumentation in the cytoplasm of these cells.

Detection of apoptosis levels in recombinant VZV-infected corneal fibroblasts. Several alphaherpesvirus US3 kinases orthologous to ORF66 have been shown to block apoptosis in response to both the stress of viral infection and to exogenous agents or treatments. Recent studies have indicated that ORF66 inhibits apoptosis in VZV-infected T cells (58), as a fraction of cells infected with VZV lacking ORF66 show higher levels of caspase-3 activation (57). In the context of the corneal stroma, keratocytes are highly sensitive to apoptosis following injury (35, 66, 67). To test the role of apoptosis in the PCF cell-specific growth requirement for ORF66, we assessed MRC-5 or PCF infected cells for the early apoptosis marker Annexin V and the viability stain 7-AAD. Gating for GFP fluorescence enabled assessment of VZV-infected cells in which the ORF66 promoter was active (Fig. 7). In MRC-5 cells infected with VZV.GFP-66, indicators of apoptosis were seen in mean levels of 6.5, 10.5, and 18.9% of GFP-expressing cells at 24, 48, and 72 h p.i., respectively. Cells infected with VZV.GFP66-kd displayed almost equivalent levels (9.2, 9.5, and 18.7%), and VZV.GFP-66s levels were slightly lower (6.4, 4.8, and 13.5%, respectively). Statistical evaluation revealed no significant difference in numbers of cells showing APC-Annexin V signal between VZV.GFP-66 and the 66 kinase mutants at any time. In contrast, PCF cells infected with VZV.GFP-66kd showed significantly higher levels of apoptosis (17.5, 13.6, and 19.7%) compared to VZV.GFP-66 (8.2, 8.5, and 11.1%) at the 24- and 48-h time points, although the levels of apoptosis of cells infected with VZV.GFP-66s were not statistically significantly different at any time point (11.3, 10.5, and 14.0% at 24, 48, and 72 h p.i.). Longer times of incubation (96 h) did not result in any further increase in levels of apoptosis. Of importance, the total levels of cells undergoing apoptosis under all conditions were in the minority, as seen previously in VZV-infected T cells (57). GFP-negative cells present in VZV-infected cultures did not show variations in levels of Annexin V staining (data not shown). These results indicate that corneal fibroblasts infected with VZV lacking ORF66

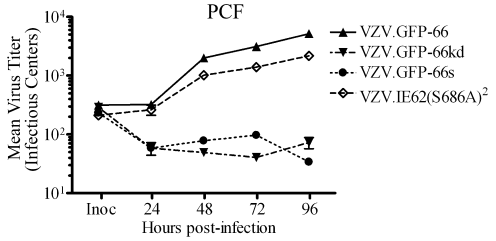

FIG. 6. Progeny growth curves of VZV.IE62(S686A)^2, VZV.GFP-66, and ORF66 mutants in PCF cells. Growth curves were determined as detailed in the legend for Fig. 2, using confluent PCF cell monolayers infected with VZV.GFP-66, VZV.GFP-66kd, VZV.GFP-66s, or VZV.IE62(S686A)^2 after infection at an MOI of 0.001. To quantify plaques of VZV.IE62(S686A)^2, cells were fixed in 4% paraformaldehyde at 4 to 5 days p.i., permeabilized, and immunostained with primary rabbit anti-62 antibodies so that plaques could be enumerated using fluorescent microscopy. Inoculant data values represent direct seeding onto MeWo cells on the same day PCF cells were infected. The *x*-axis values represent hours p.i. when cells were harvested, and *y*-axis values represent infectious centers. Each data point was done in quadruplicate and represents the mean ± standard error of these values. Growth curves are representative of two independent experiments.

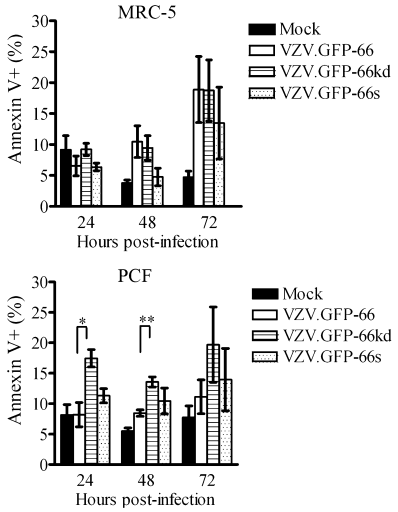

FIG. 7. Apoptosis in VZV PCF and MRC-5 cells infected with VZV and kinase-negative mutants. MRC-5 (top) and PCF cells (bottom) were infected at an MOI of 0.02 with VZV.GFP-66, VZV.GFP-66kd, or VZV.GFP-66s or mock infected. At 24, 48, and 72 h p.i., cells were carefully harvested and stained with APC-Annexin V and the viability stain 7-AAD. Cells for analysis were gated on GFP-positive cells for infection. The *x* axis shows the fraction of GFP-positive cells that stained APC-Annexin V positive as a percentage of total GFP-positive cells. Results represent means ± standard errors of values from three separate but identical experiments. Statistical analysis was done with Student's *t* test. Asterisks represent the level of statistical significance: *, $P < 0.05$; **, $P < 0.001$ compared to VZV.GFP-66 values.

kinase activity do not have dramatically increased levels of apoptosis, although the increased levels of apoptosis in VZV.GFP-66kd may be a contributing factor to its growth phenotype. We conclude that apoptosis cannot fully account for the almost complete loss of viral growth in this cell type.

DISCUSSION

In this work, we report the first nonlymphocytic cell line in which the ORF66 protein kinase is required for efficient VZV replication. We also show that ORF66 kinase-mediated phosphorylation of IE62 residue S686 is necessary and sufficient for IE62 cytoplasmic accumulation and virion packaging in the context of VZV infection. However, this activity is not the PCF cell-specific requirement for the kinase. Our data also indicate that the loss of the protein kinase does not result in a marked increase in VZV-induced apoptosis in the cell types studied, although it might contribute to growth impairment of VZV.GFP-66kd in PCF cells. Therefore, the ORF66 protein kinase has at least one additional critical role in VZV infection of this cell type.

This work contributes to the changing concept that ORF66 is required for VZV growth in certain cell types. It can thus be grouped with additional VZV genes that, when deleted, result in VZV with cell-type-specific or conditional growth patterns, including gI (10), ORF17 (56), ORF49 (55), and ORF63 (9). In addition, it has become clear that many VZV genes deemed not essential for VZV growth in cultured cells are, nevertheless, required for VZV growth in human tissue in SCID-hu mouse models of pathogenesis. An example is gI, which is not required for VZV growth in MeWo cells but is needed for growth in Vero cells and for efficient VZV replication in skin and T cells in the SCID-hu mouse model (36). A second example is the nonessential ORF10 gene, orthologous to the VP16 of HSV-1, which is required for growth in human skin implants (7). Third, deletion of the ORF47 kinase does not affect growth in culture, even though abnormal virions are formed. Such viruses show severe impairment of VZV growth in both T cell (37, 38, 60) and skin (6) implants in SCID-hu mice. Regarding ORF66, while its disruption was initially reported to have no influence on growth of the VZV vaccine strain in cultured MeWo cells (19), its disruption in the pOka background marginally reduced replication in this cell type (57). As such, it was not unexpected to find that our mutants disrupted for ORF66 kinase expression exhibited reduced cell-to-cell spread and infectious virus yields in MRC-5 cells (15). The additional VZV construct detailed here expressing complete but kinase-inactive ORF66 protein also has some growth impairment in MRC-5 cells. However, the lack of growth in human corneal fibroblasts of ORF66 kinase-negative VZV was not expected and highlights important cell-type-specific functions for the kinase. Our data suggest that ORF66 kinase-negative mutants are able to enter PCF cells, as we detected small foci of infection in which both IE62 and the ORF66 kinase were expressed. This suggests the block is at a later stage of the infectious cycle after early gene expression. Previously, it was shown that viruses disrupted for ORF66 expression or kinase activity by mutation of the ATP binding region (G102A) abrogated virus replication in T cells in the SCID-hu thy/liv mouse model (57) and in cultured T cells (60). It was further demonstrated that functional ORF66 was needed to modulate host cell signaling pathways in vitro in human tonsillar $CD4^+$ T cells, which have been proposed to be involved in the transfer of infectious virus from circulation to sites on the skin in this mouse model of VZV pathogenesis (30). We conclude that the important ORF66-encoded function involves the unique short kinase phosphorylating host or viral proteins in PCF cells. Identification of an easily cultured nonlymphocytic cell type in which the kinase is required opens up avenues to investigate these targets.

Since the PCF-specific function of ORF66 likely involves phosphorylation of a target, it was logical to investigate the only well-defined target, IE62. Our work confirmed that S686 was the critical residue by which the kinase induces cytoplasmic IE62 in the context of VZV infections and established its importance in the assembly and packaging of IE62 into virions. We also established that virion incorporation of proteins encoded by ORFs 4, 9, 10, 47, and 63 does not require IE62 in the tegument for packaging. The proteins from ORFs 4, 9, 47, and 63 have been suggested to physically interact with IE62, but it seems unlikely that these interactions with IE62 are required for their virion incorporation. The increased levels of ORF9 and ORF63 in the virion in the absence of structural IE62 are reminiscent of several reports in which absence of one tegument protein is compensated by an increase in the incorporation of other tegument components (33) or even host proteins, such as actin (34). McKnight et al., in their investigation of the essential α-TIF tegument protein, speculated that protein-protein interactions in the tegument allow a certain level of flex-

ibility of packaging and noted that larger virion-fusion protein mutants were still packaged into virions (33).

Our work has separated ORF66 phosphorylation of IE62 S686 from the PCF cell-specific function of the kinase. VZV.IE62(S686A)[2] expressed a functional kinase but showed the IE62 phenotypes of ORF66-negative VZV, yet displayed only slightly diminished growth by 96 h. This also suggests that IE62 tegument inclusion is not required for viral growth in PCF cells. A similar conclusion was proposed from studies in tonsillar T cells, such that the ORF66 function critical for VZV growth is independent of its effects on IE62. It was reported that in T cells, IE62 locates to the cytoplasm in VZV ORF66 stop or ORF66 kinase-inactive mutants (57). This suggests that IE62 subcellular localization is controlled by an ORF66-independent mechanism in tonsillar T cells, possibly a cellular kinase that regulates IE62 nuclear import. It is not known if IE62 incorporates into virions from T cells infected with ORF66-deficient VZV.

We also showed that the disruption of the kinase does not result in greatly increased levels of apoptosis in PCF cells that would account for the loss of VZV replication. Modulation of apoptotic pathways seems to be conserved for many alphaherpesvirus US3 kinases, although the mechanisms have not been fully elucidated. It has been suggested that the kinase enables maintenance of survival of the infected cell long enough to allow virion production and spread (2). Keratocytes are known to be highly susceptible to apoptosis in the corneal stroma, particularly following a corneal wound or infection (67). Our data show that stromal fibroblasts derived from corneas show only significantly more apoptosis at 24 and 48 h following infection with VZV expressing the kinase-dead protein. The fraction of cells showing apoptosis are similar to that seen in T cells (57). However, unlike that study, we found that the levels of apoptosis in VZV expressing ORF66 stop mutants were not significantly different from those in cells infected by VZV with functional kinase. The significantly higher apoptosis in VZV.GFP-66kd-infected PCF cells may reflect binding of the kinase-dead protein to a prosurvival factor that is normally phosphorylated, leading to dominant negative effects. Interestingly, in HSV-1, antiapoptotic activity stems from the amino terminus of US3 in transfected cells induced for programmed cell death (49, 51). Thus, while ORF66 kinase activity may have a role in inhibition of apoptosis in PCF, it is unlikely to be the ORF66 function responsible for the severe growth deficiency of VZV lacking functional ORF66 in PCF cells.

The critical target(s) of the kinase in this cell type remains to be defined, and our current studies are aimed at determining if the VZV kinase shares the same functions attributed to other alphaherpesvirus US3 kinases. The US3 kinases of HSV-1, Marek's disease virus, and PRV have been implied to modulate the nuclear membrane to facilitate de-envelopment of nucleocapsids into the cytoplasm, since absence of US3 kinases causes irregular nucleocapsid accumulations in the perinuclear space (27, 53, 54, 59, 64). It has been suggested that phosphorylation of lamin A/C and emerin hyperphosphorylation aid in nuclear lamina breakdown (31, 41) that is required for proper virion nuclear egress. Our recent studies (A. J. Eisfeld and P. R. Kinchington, unpublished studies) indicate that nuclear rim concentrates of GFP-66kd colocalize with nucleocapsid proteins. Work by Schaap-Nutt et al. suggests that complete virion formation is not affected in T cells infected with VZV encoding ORF66 stop mutants, and there is no similar nucleocapsid accumulation in the perinuclear regions (58). Rather, they reported lower levels of nucleocapsids in infected cells. It is possible that in PCF cells the kinase may have a more important role in virion egress than in T cells, and studies are ongoing using the GFP tag to sort and concentrate the initially infected PCF cells for electron microscopy studies of nucleocapsid maturation at the nuclear membrane.

It is possible that the ORF66 kinase augments activity of a cellular protein kinase which has different levels of activation or expression in different cell types. The US3 kinase of HSV-1 overlaps the targets of protein kinase A, which may be reduced in PCF cells (3). ORF66 also modulates the induction of the IFN pathway, as the level of Stat1 phosphorylation in a small fraction of tonsillar T cells is higher in response to IFN-γ when the kinase is not expressed (58). In SCID-hu mouse skin xenografts, VZV lesions are surrounded by a defined region of uninfected epidermal cells positive for Stat1 phosphorylation (triggered in the IFN signaling pathway), yet actual VZV-containing lesions downregulate IFN-α (30). Although ORF66 only has a modest effect on VZV titers in skin xenografts infected with pOka VZV66 stop mutants (58), it is thought that inhibition of IFN signal transduction may promote the survival of infected tonsillar T cells. Thus, it is possible that PCF cells express higher levels of IFN and that this may exert an antiviral effect. Human corneal epithelial cells have been found to increase transcriptional expression of various cytokines, including IFN-β, in response to HSV-1 infection in vitro (32). Interestingly, addition of recombinant human IFN-α2a can inhibit VZV replication in human corneal stromal fibroblast cultures (52). Investigation of the role of interferon pathway modulation by ORF66 in PCF cells is an area under study.

In conclusion, VZV deficient in functional ORF66 protein kinase expression is severely growth impaired in human corneal stromal fibroblasts, but this is not due to the kinase-mediated phosphorylation of IE62 residue S686, which drives cytoplasmic accumulation and virion packaging of IE62. While our data suggest that there is a role for ORF66 in inhibition of virus-induced apoptosis in PCF cells, this effect seems unlikely to be solely responsible for the complete growth deficiency. This work establishes that ORF66 may be critical for productive VZV growth in some nonlymphocytic cell types, and additional primary cell cultures are now being explored.

ACKNOWLEDGMENTS

This work was supported by Public Health Service grant EY09397 (P.R.K.), AI060843 (N.O.), CORE grant for vision research EY08098 (P.R.K.), funds from The Eye & Ear Foundation of Pittsburgh and Research to Prevent Blindness, Inc., and an NIH predoctoral T32 training grant AI060525 (A.E.).

We thank Kira L. Lathrop, Nancy B. Zurowski, and Jennifer L. Koury of the University of Pittsburgh Department of Ophthalmology Core modules for technical assistance with epifluorescence imaging, flow cytometry, and corneal tissue culture, respectively.

REFERENCES

1. **Abendroth, A., I. Lin, B. Slobedman, H. Ploegh, and A. M. Arvin.** 2001. Varicella-zoster virus retains major histocompatibility complex class I proteins in the Golgi compartment of infected cells. J. Virol. **75:**4878–4888.
2. **Aubert, M., and J. A. Blaho.** 2001. Modulation of apoptosis during herpes simplex virus infection in human cells. Microbes Infect. **3:**859–866.
3. **Benetti, L., and B. Roizman.** 2004. Herpes simplex virus protein kinase US3

activates and functionally overlaps protein kinase A to block apoptosis. Proc. Natl. Acad. Sci. USA **101:**9411–9416.
4. **Benetti, L., and B. Roizman.** 2007. In transduced cells, the US3 protein kinase of herpes simplex virus 1 precludes activation and induction of apoptosis by transfected procaspase 3. J. Virol. **81:**10242–10248.
5. **Besser, J., M. Ikoma, K. Fabel, M. H. Sommer, L. Zerboni, C. Grose, and A. M. Arvin.** 2004. Differential requirement for cell fusion and virion formation in the pathogenesis of varicella-zoster virus infection in skin and T cells. J. Virol. **78:**13293–13305.
6. **Besser, J., M. H. Sommer, L. Zerboni, C. P. Bagowski, H. Ito, J. Moffat, C. C. Ku, and A. M. Arvin.** 2003. Differentiation of varicella-zoster virus ORF47 protein kinase and IE62 protein binding domains and their contributions to replication in human skin xenografts in the SCID-hu mouse. J. Virol. **77:** 5964–5974.
7. **Che, X., L. Zerboni, M. H. Sommer, and A. M. Arvin.** 2006. Varicella-zoster virus open reading frame 10 is a virulence determinant in skin cells but not in T cells in vivo. J. Virol. **80:**3238–3248.
8. **Cilloniz, C., W. Jackson, C. Grose, D. Czechowski, J. Hay, and W. T. Ruyechan.** 2007. The varicella-zoster virus (VZV) ORF9 protein interacts with the IE62 major VZV transactivator. J. Virol. **81:**761–774.
9. **Cohen, J. I., T. Krogmann, S. Bontems, C. Sadzot-Delvaux, and L. Pesnicak.** 2005. Regions of the varicella-zoster virus open reading frame 63 latency-associated protein important for replication in vitro are also critical for efficient establishment of latency. J. Virol. **79:**5069–5077.
10. **Cohen, J. I., and H. Nguyen.** 1997. Varicella-zoster virus glycoprotein I is essential for growth of virus in Vero cells. J. Virol. **71:**6913–6920.
11. **Cohen, J. I., and S. E. Straus.** 2001. Varicella-zoster virus and its replication, p. 2707–2729. *In* D. M. Knipe, P. M. Howley, D. E. Griffin, R. A. Lamb, M. A. Martin, B. Roizman, and S. E. Straus (ed.), Fields virology, 4th ed. Lippincott Williams & Wilkins, Philadelphia, PA.
12. **Deruelle, M., K. Geenen, H. J. Nauwynck, and H. W. Favoreel.** 2007. A point mutation in the putative ATP binding site of the pseudorabies virus US3 protein kinase prevents Bad phosphorylation and cell survival following apoptosis induction. Virus Res. **128:**65–70.
13. **Disney, G. H., and R. D. Everett.** 1990. A herpes simplex virus type 1 recombinant with both copies of the Vmw175 coding sequences replaced by the homologous varicella-zoster virus open reading frame. J. Gen. Virol. **71:**2681–2689.
14. **Eisfeld, A. J., S. E. Turse, S. A. Jackson, E. C. Lerner, and P. R. Kinchington.** 2006. Phosphorylation of the varicella-zoster virus (VZV) major transcriptional regulatory protein IE62 by the VZV open reading frame 66 protein kinase. J. Virol. **80:**1710–1723.
15. **Eisfeld, A. J., M. B. Yee, A. Erazo, A. Abendroth, and P. R. Kinchington.** 2007. Downregulation of class I major histocompatibility complex surface expression by varicella-zoster virus involves open reading frame 66 protein kinase-dependent and -independent mechanisms. J. Virol. **81:**9034–9049.
16. **Favoreel, H. W., G. Van Minnebruggen, D. Adriaensen, and H. J. Nauwynck.** 2005. Cytoskeletal rearrangements and cell extensions induced by the US3 kinase of an alphaherpesvirus are associated with enhanced spread. Proc. Natl. Acad. Sci. USA **102:**8990–8995.
17. **Felser, J. M., P. R. Kinchington, G. Inchauspe, S. E. Straus, and J. M. Ostrove.** 1988. Cell lines containing varicella-zoster virus open reading frame 62 and expressing the "IE" 175 protein complement ICP4 mutants of herpes simplex virus type 1. J. Virol. **62:**2076–2082.
18. **Heineman, T. C., and J. I. Cohen.** 1995. The varicella-zoster virus (VZV) open reading frame 47 (ORF47) protein kinase is dispensable for viral replication and is not required for phosphorylation of ORF63 protein, the VZV homolog of herpes simplex virus ICP22. J. Virol. **69:**7367–7370.
19. **Heineman, T. C., K. Seidel, and J. I. Cohen.** 1996. The varicella-zoster virus ORF66 protein induces kinase activity and is dispensable for viral replication. J. Virol. **70:**7312–7317.
20. **Hu, H., and J. I. Cohen.** 2005. Varicella-zoster virus open reading frame 47 (ORF47) protein is critical for virus replication in dendritic cells and for spread to other cells. Virology **337:**304–311.
21. **Kinchington, P. R., D. Bookey, and S. E. Turse.** 1995. The transcriptional regulatory proteins encoded by varicella-zoster virus open reading frames (ORFs) 4 and 63, but not ORF 61, are associated with purified virus particles. J. Virol. **69:**4274–4282.
22. **Kinchington, P. R., K. Fite, A. Seman, and S. E. Turse.** 2001. Virion association of IE62, the varicella-zoster virus (VZV) major transcriptional regulatory protein, requires expression of the VZV open reading frame 66 protein kinase. J. Virol. **75:**9106–9113.
23. **Kinchington, P. R., K. Fite, and S. E. Turse.** 2000. Nuclear accumulation of IE62, the varicella-zoster virus (VZV) major transcriptional regulatory protein, is inhibited by phosphorylation mediated by the VZV open reading frame 66 protein kinase. J. Virol. **74:**2265–2277.
24. **Kinchington, P. R., J. K. Hougland, A. M. Arvin, W. T. Ruyechan, and J. Hay.** 1992. The varicella-zoster virus immediate-early protein IE62 is a major component of virus particles. J. Virol. **66:**359–366.
25. **Kinchington, P. R., G. Inchauspe, J. H. Subak-Sharpe, F. Robey, J. Hay, and W. T. Ruyechan.** 1988. Identification and characterization of a varicella-zoster virus DNA-binding protein by using antisera directed against a predicted synthetic oligopeptide. J. Virol. **62:**802–809.
26. **Kinchington, P. R., and S. E. Turse.** 1998. Regulated nuclear localization of the varicella-zoster virus major regulatory protein, IE62. J. Infect. Dis. **178**(Suppl. 1)**:**S16–S21.
27. **Klupp, B. G., H. Granzow, and T. C. Mettenleiter.** 2001. Effect of the pseudorabies virus US3 protein on nuclear membrane localization of the UL34 protein and virus egress from the nucleus. J. Gen. Virol. **82:**2363–2371.
28. **Ku, C. C., J. Besser, A. Abendroth, C. Grose, and A. M. Arvin.** 2005. Varicella-zoster virus pathogenesis and immunobiology: new concepts emerging from investigations with the SCIDhu mouse model. J. Virol. **79:** 2651–2658.
29. **Ku, C. C., J. A. Padilla, C. Grose, E. C. Butcher, and A. M. Arvin.** 2002. Tropism of varicella-zoster virus for human tonsillar $CD4^+$ T lymphocytes that express activation, memory, and skin homing markers. J. Virol. **76:** 11425–11433.
30. **Ku, C. C., L. Zerboni, H. Ito, B. S. Graham, M. Wallace, and A. M. Arvin.** 2004. Varicella-zoster virus transfer to skin by T Cells and modulation of viral replication by epidermal cell interferon-alpha. J. Exp. Med. **200:**917–925.
31. **Leach, N., S. L. Bjerke, D. K. Christensen, J. M. Bouchard, F. Mou, R. Park, J. Baines, T. Haraguchi, and R. J. Roller.** 2007. Emerin is hyperphosphorylated and redistributed in herpes simplex virus type 1-infected cells in a manner dependent on both UL34 and US3. J. Virol. **81:**10792–10803.
32. **Li, H., J. Zhang, A. Kumar, M. Zheng, S. S. Atherton, and F. S. Yu.** 2006. Herpes simplex virus 1 infection induces the expression of proinflammatory cytokines, interferons and TLR7 in human corneal epithelial cells. Immunology **117:**167–176.
33. **McKnight, J. L., M. Doerr, and Y. Zhang.** 1994. An 85-kilodalton herpes simplex virus type 1 alpha *trans*-induction factor (VP16)-VP13/14 fusion protein retains the transactivation and structural properties of the wild-type molecule during virus infection. J. Virol. **68:**1750–1757.
34. **Michael, K., B. G. Klupp, T. C. Mettenleiter, and A. Karger.** 2006. Composition of pseudorabies virus particles lacking tegument protein US3, UL47, or UL49 or envelope glycoprotein E. J. Virol. **80:**1332–1339.
35. **Miles, D. H., M. D. Willcox, and S. Athmanathan.** 2004. Ocular and neuronal cell apoptosis during HSV-1 infection: a review. Curr. Eye Res. **29:**79–90.
36. **Moffat, J., H. Ito, M. Sommer, S. Taylor, and A. M. Arvin.** 2002. Glycoprotein I of varicella-zoster virus is required for viral replication in skin and T cells. J. Virol. **76:**8468–8471.
37. **Moffat, J. F., M. D. Stein, H. Kaneshima, and A. M. Arvin.** 1995. Tropism of varicella-zoster virus for human $CD4^+$ and $CD8^+$ T lymphocytes and epidermal cells in SCID-hu mice. J. Virol. **69:**5236–5242.
38. **Moffat, J. F., L. Zerboni, M. H. Sommer, T. C. Heineman, J. I. Cohen, H. Kaneshima, and A. M. Arvin.** 1998. The ORF47 and ORF66 putative protein kinases of varicella-zoster virus determine tropism for human T cells and skin in the SCID-hu mouse. Proc. Natl. Acad. Sci. USA **95:**11969–11974.
39. **Morris, J. B., H. Hofemeister, and P. O'Hare.** 2007. Herpes simplex virus infection induces phosphorylation and delocalization of emerin, a key inner nuclear membrane protein. J. Virol. **81:**4429–4437.
40. **Morrow, G., B. Slobedman, A. L. Cunningham, and A. Abendroth.** 2003. Varicella-zoster virus productively infects mature dendritic cells and alters their immune function. J. Virol. **77:**4950–4959.
41. **Mou, F., T. Forest, and J. D. Baines.** 2007. US3 of herpes simplex virus type 1 encodes a promiscuous protein kinase that phosphorylates and alters localization of lamin A/C in infected cells. J. Virol. **81:**6459–6470.
42. **Muller, L. J., L. Pels, and G. F. Vrensen.** 1995. Novel aspects of the ultrastructural organization of human corneal keratocytes. Investig. Ophthalmol. Vis. Sci. **36:**2557–2567.
43. **Murata, T., F. Goshima, Y. Yamauchi, T. Koshizuka, H. Takakuwa, and Y. Nishiyama.** 2002. Herpes simplex virus type 2 US3 blocks apoptosis induced by sorbitol treatment. Microbes Infect. **4:**707–712.
44. **Ng, T. I., L. Keenan, P. R. Kinchington, and C. Grose.** 1994. Phosphorylation of varicella-zoster virus open reading frame (ORF) 62 regulatory product by viral ORF 47-associated protein kinase. J. Virol. **68:**1350–1359.
45. **Ogg, P. D., P. J. McDonell, B. J. Ryckman, C. M. Knudson, and R. J. Roller.** 2004. The HSV-1 Us3 protein kinase is sufficient to block apoptosis induced by overexpression of a variety of Bcl-2 family members. Virology **319:**212–224.
46. **Pavan-Langston, D.** 2000. Ophthalmic zoster, p. 276–298. *In* A. Arvin and A. Gershon (ed.), Varicella-zoster virus: virology and clinical management. Cambridge University Press, Cambridge, United Kingdom.
47. **Perera, L. P., J. D. Mosca, W. T. Ruyechan, G. S. Hayward, S. E. Straus, and J. Hay.** 1993. A major transactivator of varicella-zoster virus, the immediate-early protein IE62, contains a potent N-terminal activation domain. J. Virol. **67:**4474–4483.
48. **Perera, L. P., J. D. Mosca, M. Sadeghi-Zadeh, W. T. Ruyechan, and J. Hay.** 1992. The varicella-zoster virus immediate early protein, IE62, can positively regulate its cognate promoter. Virology **191:**346–354.
49. **Poon, A. P., L. Benetti, and B. Roizman.** 2006. U_S3 and $U_S3.5$ protein kinases of herpes simplex virus 1 differ with respect to their functions in blocking apoptosis and in virion maturation and egress. J. Virol. **80:**3752–3764.

50. **Poon, A. P., H. Gu, and B. Roizman.** 2006. ICP0 and the US3 protein kinase of herpes simplex virus 1 independently block histone deacetylation to enable gene expression. Proc. Natl. Acad. Sci. USA **103:**9993–9998.
51. **Poon, A. P., and B. Roizman.** 2007. Mapping of key functions of the herpes simplex virus 1 U_S3 protein kinase: the U_S3 protein can form functional heteromultimeric structures derived from overlapping truncated polypeptides. J. Virol. **81:**1980–1989.
52. **Punda-Polic, V., W. J. O'Brien, and J. L. Taylor.** 1999. Synergistic antivaricella-zoster virus activity of interferon-alpha 2a and acyclovir in corneal cells. Zentralbl. Bakteriol. **289:**203–210.
53. **Reynolds, A. E., E. G. Wills, R. J. Roller, B. J. Ryckman, and J. D. Baines.** 2002. Ultrastructural localization of the herpes simplex virus type 1 UL31, UL34, and US3 proteins suggests specific roles in primary envelopment and egress of nucleocapsids. J. Virol. **76:**8939–8952.
54. **Ryckman, B. J., and R. J. Roller.** 2004. Herpes simplex virus type 1 primary envelopment: UL34 protein modification and the US3-UL34 catalytic relationship. J. Virol. **78:**399–412.
55. **Sadaoka, T., H. Yoshii, T. Imazawa, K. Yamanishi, and Y. Mori.** 2007. Deletion in open reading frame 49 of varicella-zoster virus reduces virus growth in human malignant melanoma cells but not in human embryonic fibroblasts. J. Virol. **81:**12654–12665.
56. **Sato, H., L. D. Callanan, L. Pesnicak, T. Krogmann, and J. I. Cohen.** 2002. Varicella-zoster virus (VZV) ORF17 protein induces RNA cleavage and is critical for replication of VZV at 37 degrees C but not 33 degrees C. J. Virol. **76:**11012–11023.
57. **Schaap-Nutt, A., M. Sommer, X. Che, L. Zerboni, and A. M. Arvin.** 2006. ORF66 protein kinase function is required for T-cell tropism of varicella-zoster virus in vivo. J. Virol. **80:**11806–11816.
58. **Schaap, A., J. F. Fortin, M. Sommer, L. Zerboni, S. Stamatis, C. C. Ku, G. P. Nolan, and A. M. Arvin.** 2005. T-cell tropism and the role of ORF66 protein in pathogenesis of varicella-zoster virus infection. J. Virol. **79:**12921–12933.
59. **Schumacher, D., B. K. Tischer, S. Trapp, and N. Osterrieder.** 2005. The protein encoded by the US3 orthologue of Marek's disease virus is required for efficient de-envelopment of perinuclear virions and involved in actin stress fiber breakdown. J. Virol. **79:**3987–3997.
60. **Soong, W., J. C. Schultz, A. C. Patera, M. H. Sommer, and J. I. Cohen.** 2000. Infection of human T lymphocytes with varicella-zoster virus: an analysis with viral mutants and clinical isolates. J. Virol. **74:**1864–1870.
61. **Spengler, M., N. Niesen, C. Grose, W. T. Ruyechan, and J. Hay.** 2001. Interactions among structural proteins of varicella zoster virus. Arch. Virol. Suppl. **17:**71–79.
62. **Tischer, B. K., B. B. Kaufer, M. Sommer, F. Wussow, A. M. Arvin, and N. Osterrieder.** 2007. A self-excisable infectious bacterial artificial chromosome clone of varicella-zoster virus allows analysis of the essential tegument protein encoded by ORF9. J. Virol. **81:**13200–13208.
63. **Tischer, B. K., J. von Einem, B. Kaufer, and N. Osterrieder.** 2006. Two-step red-mediated recombination for versatile high-efficiency markerless DNA manipulation in Escherichia coli. BioTechniques **40:**191–197.
64. **Wagenaar, F., J. M. Pol, B. Peeters, A. L. Gielkens, N. de Wind, and T. G. Kimman.** 1995. The US3-encoded protein kinase from pseudorabies virus affects egress of virions from the nucleus. J. Gen. Virol. **76:**1851–1859.
65. **Wenkel, H., C. Rummelt, V. Rummelt, G. Jahn, B. Fleckenstein, and G. O. Naumann.** 1993. Detection of varicella zoster virus DNA and viral antigen in human cornea after herpes zoster ophthalmicus. Cornea **12:**131–137.
66. **West-Mays, J. A., and D. J. Dwivedi.** 2006. The keratocyte: corneal stromal cell with variable repair phenotypes. Int. J. Biochem. Cell. Biol. **38:**1625–1631.
67. **Wilson, S. E.** 2000. Role of apoptosis in wound healing in the cornea. Cornea **19:**S7–S12.
68. **Yang, M., H. Peng, J. Hay, and W. T. Ruyechan.** 2006. Promoter activation by the varicella-zoster virus major transactivator IE62 and the cellular transcription factor USF. J. Virol. **80:**7339–7353.